

Sessile and Pendant Micro-Liter Drops Evaporate at Different Rates: An Experimental Approach

M. Moore¹, A. Amirfazli², and S. Farshid Chini^{3*}

¹Department of Mechanical Engineering, University of Alberta
Edmonton, AB, T6G 2G8, Canada.

²Department of Mechanical Engineering, York University
Toronto, ON, M3J 1P3, Canada.

³Department of Mechanical Engineering, University of Tehran
Tehran, 1417613131, Iran.

Received: 3 Apr. 2016 , Accepted: 30 May 2016

Abstract

Evaporation of micro-liter drops from solid surfaces at room condition is mainly governed by diffusion. Therefore, there should be no difference between evaporation rate of sessile and pendant drops. However, some studies indicate a difference and explain the difference using buoyancy. The objective here is to reconcile the inconsistency in the literature. For that, first, by comparing two identical suspended drops, one with a plate on top and the other underneath with a space between drop and plate, we showed the contribution of buoyancy in evaporation is at most less than 8%. When a plate was placed on top, water (its vapor is lighter than air) evaporated slower and hydrocarbons (their vapors are heavier than air) evaporated faster. Interestingly, it was observed when drops touch the plates (i.e. sessile and pendant drops), both water and hydrocarbon drops evaporated faster in sessile configuration. The observation for hydrocarbons is in contradiction with what buoyancy explains. To describe the difference, different scenarios were studied. It was found that sessile drops stay longer in the “constant wetted area” (CWA) mode, before switching to the CCA (constant contact angle) mode, e.g. a 4 μl sessile water drop on a Poly(methyl methacrylate) coated silicon stays in the CWA mode for 318 s whereas for a similar pendant drop this time is 274 s. Considering the fact that evaporation rate in the CWA mode is 30–40% higher compared to the CCA mode, the faster evaporation rate of sessile drops may be explained.

Keywords:

Evaporation, drop, buoyancy, sessile, pendant, diffusion, evaporation modes

1. Introduction

Drop evaporation from a solid surface is of interest in ink-jet printing [1,2], spraying pesticides [3], thin film coating [4], spray cooling [5], and micro/nano

fabrication [6]. In all of these applications, controlling the evaporation rate is important. The main goal of this study is to see if there is a significant difference between evaporation rate of sessile and pendant drops; and explain the difference, if there is any. This study

* Corresponding author e-mail: chini@ut.ac.ir

provides further insight into the process of drop evaporation. To isolate the effect of other parameters, the study is limited to micro-liter drops at room temperature, atmospheric pressure, and quiescence.

Evaporation models accurately estimate the evaporation rate of micro-liter drops; however, they reflect no difference between evaporation rate of sessile and pendant drops [7]. According to the evaporation models, evaporation is limited by vapor transport (diffusion and convection) from the drop surface and not phase change [8-11]. Pure-diffusive models [9] use Maxwell's assumptions (i.e. convection is negligible, and process is steady-state). Diffusive-convective models [12] relax the Maxwell's assumptions, but for non-volatile liquids pure-diffusive and diffusive-convective models are equivalent [12]. The flux varying models [13] suggest that due to the presence of a substrate, evaporation flux of sessile drops and suspended spherical drops are not equal. To compensate the effect of substrate, $f(\theta)$, a function of contact angle [14], is used in flux varying models.

Despite the evaporation models, some experimental studies report a difference between the evaporation rate of sessile and pendant drops (similar liquid, drop volume and substrate) e.g. [15].

Buoyancy⁶ can be a potential explanation for the difference [18-21]. In [22], using Schlieren images it was shown that a cloud-shaped vapor layer quickly forms over hydrocarbon sessile drops. This cloud stays constant and slowly spreads horizontally away from the drop. While according to diffusion, the cloud should have spread in a roughly hemispherical direction. To explain the shape of cloud, it should be noted that the vapor of hydrocarbons is heavier than air and the gravity pushes the vapor cloud down. The downward push or buoyancy-driven convection is against the gravity. Therefore, it impedes the vapor flow and evaporation of sessile drops, and accelerates the evaporation rate of pendant drops. As the vapor of water is lighter than air, the opposite is expected for water. However, in [19], evaporation rate of 3-methylpentane, hexane, cyclohexane and heptane sessile drops were studied. All of the studied liquids in [16,19] were heavier than air. It was expected that the buoyancy-driven convection slows the evaporation rate; however, the opposite was observed. To explain,

it should be noted that in both [16,19] the relation used for calculating the evaporation rate of sessile drops was the pure-diffusive model suggested for suspended spherical drops (not for sessile drops). Also, the drops with their underneath bases were raised slightly above the horizontal substrate which makes the flow of the vapor cloud on top of the sessile drops easier. In [23] by studying 0.6 to 60 mm sessile water drops on different substrates it was shown natural convection is negligible for drops with radius smaller than 20 mm.

In summary, there is no consistency in the literature to answer if there is a meaningful difference between evaporation rate of sessile and pendant drops. Also, the significance of buoyancy-driven convection is still in question.

2. EXPERIMENTAL METHODS

All experiments were performed in normal laboratory condition (pressure: 94 kPa, temperature: 21°C, and relative humidity: 40%); and temperatures of the surrounding, substrate and drop were kept uniform. The drop sizes were 4–8 μ L. Evaporation calculations were for the first half-life of the evaporation as for nano-liter drops some other factors (e.g. Kelvin effect) can take over [24]. Each experiment was repeated at least nine times and averages are presented. The performed experiments were: (i) suspended drops, (ii) sessile and pendant drops, and (iii) imaging.

3. SUSPENDED DROPS

DI water (DirectQ Millipore, 18.02 g/mol), isobutanol (Anachemia 99%, 74.12 g/mol), ethanol (Commercial Alcohols, 100%, 46.07 g/mol), and methanol (Fisher Scientific, 99.8%, 32.04 g/mol), liquids were used. A downward knot was tied on a copper wire and the drop was hung from it. Weight of the drop was measured with the system explained in the next paragraph for the three cases: (i) no plate, (ii) plate underneath the drop, and (iii) plate on top of the drop. The plate was aluminum and 1 mm gap was between drop and plate.

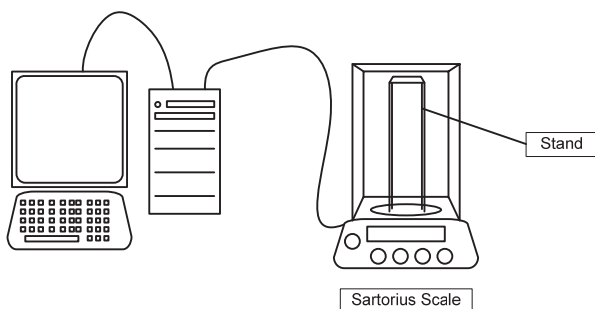
A Sartorius TE214S scale was integrated into a computer via a parallel port, which was able to give a reading every 5 seconds to a spreadsheet. The scale was put in an opaque box to mitigate radiation and airflow effects while still being large enough so that

(a) ⁶ One should not confuse buoyancy-driven convection with convection as buoyancy is caused by gravity and density variation whereas convection (or bulk motion of vapor) is not [13]. Buoyancy may change the convection and evaporation consequently [16]. The buoyancy-

driven convection in this study is solutal and not thermal. As shown in [17], when the difference between the ambient temperature and substrate is small, temperature driven buoyancy is negligible.

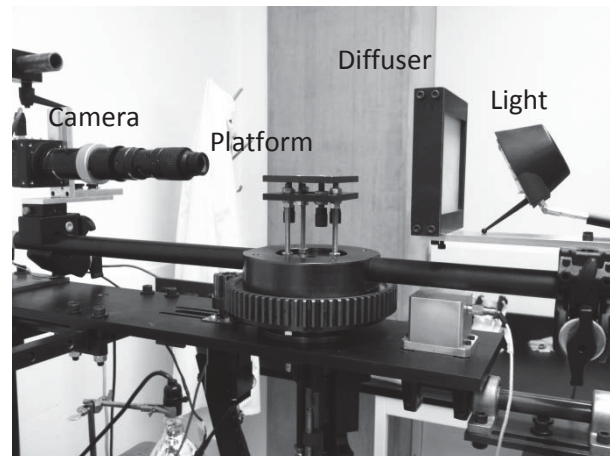
(b)

diffusion can still proceed without interference. A stand, measuring 15 cm high, was constructed to support the substrate (see Fig. 1a). This height was chosen to avoid any wall effects. A Fisher micropipette was held vertically when placing the drops. For comparing the evaporation rates, slope of drop mass (m) in time (t) was used. Regarding the slope of drop mass in time, as shown in [9], pure-diffusive models follow the 2/3 law (i.e. mass to the power of 2/3 linearly decreases in time). However, for sessile drops in the constant wetted area (CWA) mode the power



(a)

depends on the initial contact angle [25]. For the initial contact angle close to zero, the 1/1 law holds [20,25]. As the initial contact angle increases, it gets closer to the 2/3 law. For the initial contact angles larger than 150°, the power is slightly lower than 2/3 [26]. For simplicity in this study the 1/1 power is used to compare the evaporation rates. The slopes of mass in time were compared using t-test with 95% confidence level.



(b)

- (1) **Fig. 1** Experimental setup for (a) measuring the drop weight and (b) recording the drop image during evaporation are shown. The stand in (a) is for holding the substrate. An opaque box was used to limit the radiation from the room and is not shown here.

4. SESSILE AND PENDANT DROPS

DI water, as a liquid which its vapor is lighter than air (molar mass: 28.97 g/mol); and isobutanol, as a liquid which its vapor is heavier than air [27], were used. From Avogadro's law, at constant temperature, the molar volume of a gas is constant. So, the molar mass corresponds directly to density [28].

To account for possible effects of substrate, drop evaporation was studied on four different substrates: aluminum plate (25 × 49 × 1.5 mm), glass slide (26 × 76 × 1 mm), silicon wafer (Ultrasil, 20 × 44 × 0.5 mm) and poly(-methyl methacrylate), PMMA, coated silicon wafer (19 × 45 × 0.5 mm). The aluminum, glass, and silicon substrates were placed in a diluted chromo-sulfuric acid for a minimum of 24 hours and rinsed with acetone, ethanol, and distilled water, then dried under heat lamp in a chamber. To place a pendant drop, the substrate was placed on the stand and the pipette was inverted to place the drop (this was found to be the most consistent method). After each experiment, the substrates were washed with methanol

followed by acetone and rinsed with distilled water and dried using blowing nitrogen. The surfaces were kept isolated from the environment, when not in use, to avoid contamination. Air stream was used on the substrate to purge the enclosure before every experiment, to ensure all liquid was purged from the substrate and no excess vapor was trapped within the box. Silicon was chosen to be coated as it is smooth, homogeneous and rigid. The PMMA coated silicon wafer was produced as follows: PMMA powders (Aldrich®) were diluted with Toluene (Fisher Chemical) with solute concentration of 3% $\frac{w}{w}$. After spin coating at 2400 rpm, coated silicon wafers were put in an oven for 24 hours at 100°C. Roughness of the PMMA coated silicon was found to be similar to the roughness of silicon before coating, i.e. 50 ± 10 nm. Roughness was measured with Axio CSM-700 Confocal Microscope with scanning resolution of 20 nm.

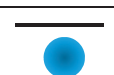
5. IMAGING

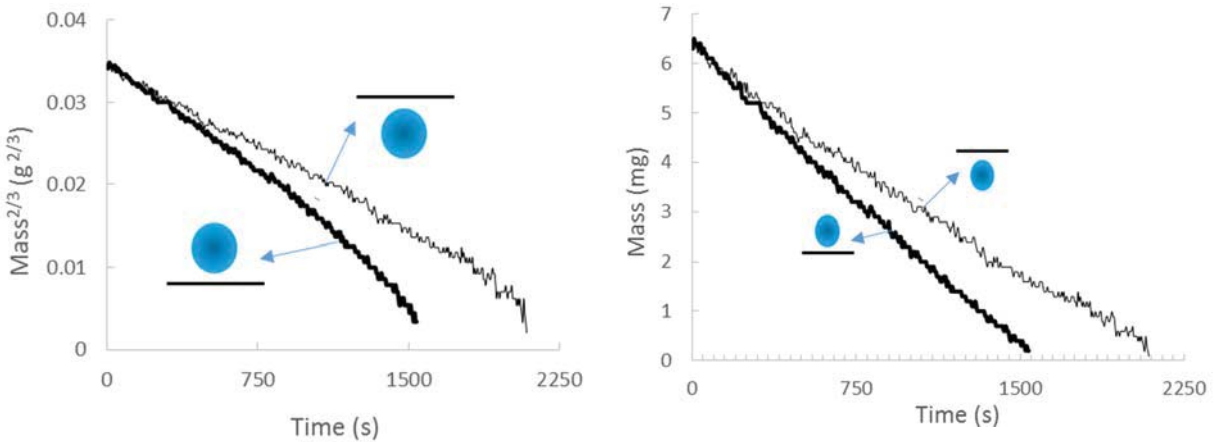
DI water was used as liquid; and aluminum, glass, silicon, and PMMA coated silicon were the substrates. Drop images were taken using Basler A302fs CCD camera attached to a Navitar 0.67X NIRA lens (see Fig. 1b). Images were processed using the in-house developed software SPPF ver. 4.2 [29]. It should be noted that the experimental environment here is not identical to the other two experiments. In order to capture images a light had to be introduced within the box, causing radiation on the sample. However, this should not be of concern as the purpose here is to qualitatively compare the evolution of shapes for sessile and pendant drops during the evaporation.

6. RESULTS AND DISCUSSION

For suspended spherical drops, as shown in Table 1, the maximum evaporation rate is when there is no plate near the drop. Placing a plate in the proximity of the drop decreases the evaporation rate. The evaporation reduction is partly due to blocking the diffusion. However, if diffusion was the only governing factor, placing the plate on top or underneath the drop should have had similar effects. When the plate was under, water drops evaporated faster; and methanol, ethanol and isobutanol (which their vapors are heavier than air) drops evaporated slower. All these differences can be explained using buoyancy.

Table 1 Slope of mass versus time ($\mu\text{g/s}$), as an indication of evaporation rate, is presented for water (as a liquid which its vapor is lighter than air), methanol, ethanol, and isobutanol (as liquids which their vapors are heavier than air), drop volumes were 4–7 μl . Drops were held in proximity of a substrate (1 mm gap between drop and plate at the beginning of the evaporation). Drop mass measurements were for the first half life and the value of R^2 for all the linear fits was larger than 0.99.

Liquid	Water	Methanol	Ethanol	Isobutanol
Initial mass (mg)	6.6 ± 0.2	4.2 ± 0.2	4.5 ± 0.2	4.6 ± 0.2
Slope of “mass” vs. “time” ($\mu\text{g/s}$)	 3.6 ± 0.1	21.0 ± 1	16.2 ± 0.3	4.8 ± 0.1
	 3.4 ± 0.2	22.7 ± 2	17.1 ± 2	5.3 ± 0.2
	 4.1 ± 0.1	25.5 ± 2	19.1 ± 1	5.9 ± 1



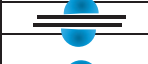
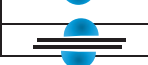
(2) **Fig. 2** Time trace of mass for a 6.4 mg suspended water drop in closeness of a solid surface is shown. For substrate on top, drop evaporation is slower (evaporation time is longer). The slopes for plate on top and plate underneath in this experiment are $3.3 \mu\text{g/s}$ and $3.6 \mu\text{g/s}$, accordingly ($R^2 = 0.99$). The inset shows $m^{2/3}$ versus time for the same experiment.

As shown in Table 1, for water drop when the plate was placed on top, evaporation rate decreased by 17% ($|4.1 - 3.4|/4.1 \times 100\%$); whereas if the same plate was underneath, the evaporation rate decreased by 12% ($|4.1 - 3.6|/4.1 \times 100\%$). The difference can be attributed to buoyancy as location of the plate does not affect the diffusion. For methanol drop when the plate was placed on top evaporation rate decreased by 11% ($|25.5 - 22.7|/25.5 \times 100\%$); and when the same plate was underneath the evaporation rate decreased by 18% ($|25.5 - 21|/25.5 \times 100\%$). Therefore, the contribution of buoyancy on evaporation of water, methanol, ethanol and isobutanol can be roughly estimated⁷ as 5% ($|3.6 - 3.4|/4.1 \times 100\%$), 7% ($|21.0 - 22.7|/28.3 \times 100\%$), 5% ($|16.2 - 17.1|/19.1 \times 100\%$), and 8%

($|4.8 - 5.3|/5.9 \times 100\%$), respectively.

For sessile and pendant drops, as shown in Table 2; independent of the liquid type and substrate, evaporation was always faster in sessile configuration. As shown in Table 2, sessile water drops on glass, silicon, PMMA coated silicon and aluminum evaporated 35% ($|6.9 - 5.1|/5.1 \times 100\%$), 24% ($|5.1 - 4.1|/4.1 \times 100\%$), 19% ($|3.7 - 3.1|/3.1 \times 100\%$), and 23% ($|2.7 - 2.2|/2.2 \times 100\%$), respectively, faster than pendant drops. Also, sessile isobutanol drops on glass, silicon, and aluminum evaporated 16% ($|8.6 - 7.4|/7.4 \times 100\%$), 18% ($|13 - 11|/11 \times 100\%$), and 30% ($|13 - 10|/10 \times 100\%$), respectively, faster than pendant drops.

Table 2 Slope of mass versus time, as an indication of evaporation rate, is presented for water (as a liquid which its vapor is lighter than air), and isobutanol (as a liquid which its vapor is heavier than air), the largest characteristic length of sessile and pendant drops was 2 mm. Isobutanol dissolves PMMA and was not included. Initial contact angle of water drops on glass, silicon, PMMA coated silicon and aluminum were 9.4o, 20.4o, 40.9o and 73.1o. There was no significance difference between contact angle of sessile and pendant drops

Substrate		Glass	Silicon	PMMA	Aluminum	
Slope of "mass" vs. "time" ($\mu\text{g/s}$)	Water		6.9 ± 0.1	5.1 ± 0.2	3.7 ± 0.1	2.7 ± 0.0
			5.1 ± 0.1	4.1 ± 0.1	3.1 ± 0.1	2.2 ± 0.1
	Isobutanol		8.6 ± 0.2	13 ± 0.5	Dissolves	13 ± 1
			7.4 ± 0.3	11 ± 0.5	Dissolves	10 ± 0.5

If diffusion was the only governing factor, sessile and pendant drops should have had equal evaporation rates (as long as both sessile and pendant drop shapes were unaffected by gravity, which is the case here, see Appendix I). Also, buoyancy-driven convection cannot explain the faster evaporation rate of sessile isobutanol drops. Even for water, buoyancy cannot explain the up to 35% faster evaporation of sessile drops. Regarding Table 2, it should be noted that the evaporation of methanol and ethanol on the substrates was very fast and finding a meaningful slope was not possible.

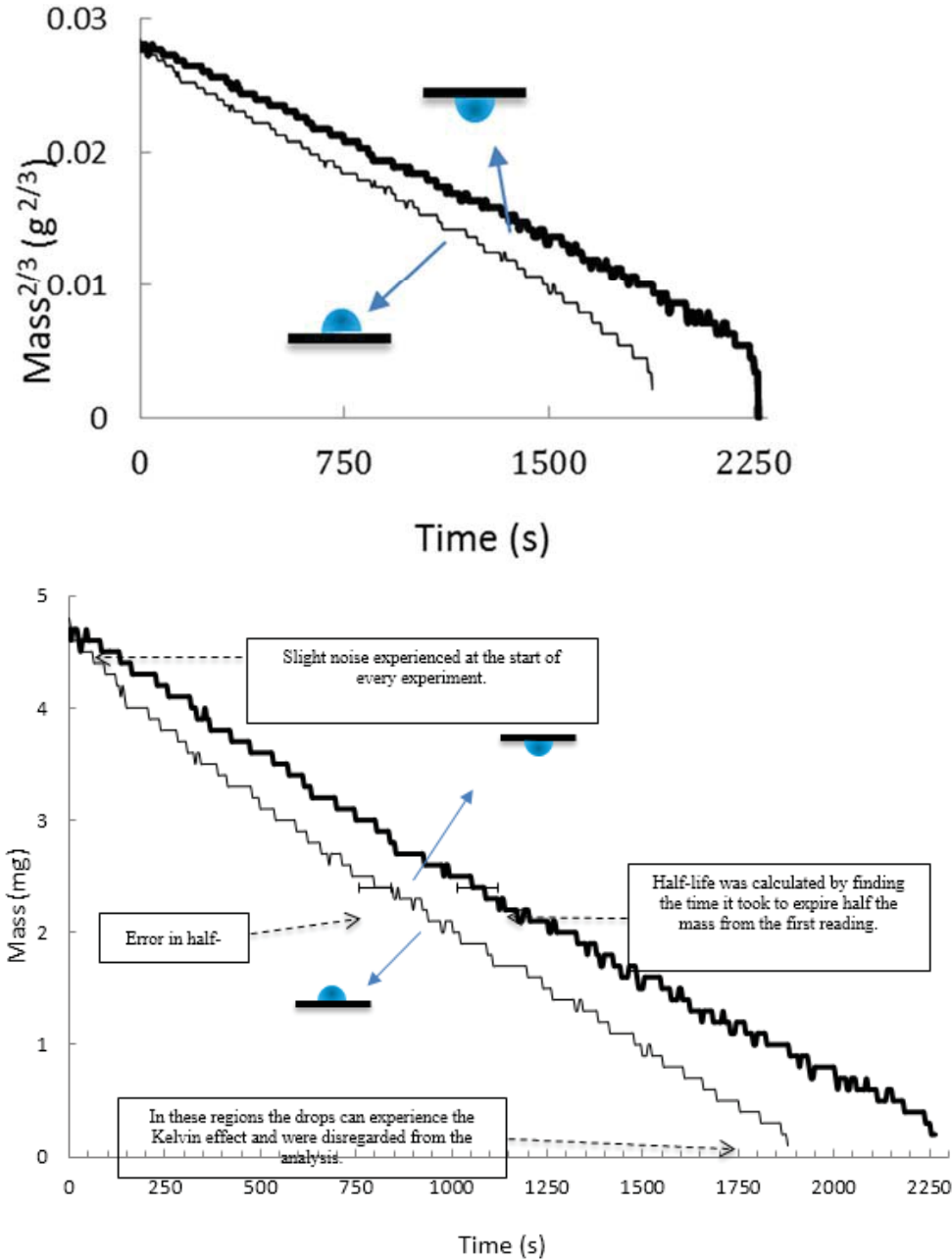
Likely such factor stems from the interaction of drop and surface. This is so, since when drops were not in contact with the plate, buoyancy could explain the evaporation rate difference.

As shown in Table 2, for the same liquid type (e.g. sessile water drops) changing the substrate changes the evaporation rate. The substrate may change the length of the contact line (through changing the contact angle), mobility of the contact line (through changing the contact angle hysteresis), and heat transfer (through changing the thermal conductivity of the

The above discussions suggest there should be another factor which overrides the effect of buoyancy.

comparing the buoyancy-driven convection with evaporation rate.

(c) ⁷ These percentages are produced only for comparing different cases. They are not proper for



(3) Fig. 3 Time trace of mass for a 4.8 mg water drop in sessile and pendant configurations on an aluminum surface is shown. It was observed that when drop is in sessile configuration, drop evaporation is faster (evaporation time is shorter). The slope of mass versus time for sessile and pendant configurations in this experiment are $2.7 \mu\text{g/s}$ and $2.2 \mu\text{g/s}$, respectively ($R^2 = 0.99$). As shown in the inset, $m^{2/3}$ versus time for the first half-life is linear as well (which is the suggested relation for pure-diffusive evaporation of spherical drops). For simplicity, we used the slope of mass versus time rather than $m^{2/3}$ versus time.

substrate) [24,30-32]. The temperature of the drop, and substrate are controlled and surface cooling for this size of drop is negligible (less than 0.02°C [33]). Also, for sessile and pendant drops, thermal conductivity of the substrate is the same. Therefore, thermal conductivity of the substrate will not be discussed.

Due to gravity, contact angle of sessile drops is slightly smaller than pendant drops [34]. However, the difference is negligible for micro-liter drops (see Appendix I). For a constant drop volume, smaller contact angle is equivalent to larger contact line and evaporation rate is higher near the contact line [35-37].

Therefore, using a substrate with lower contact angle may increase the evaporation rate, e.g. see Table 2. Although, the contact angle could explain different evaporation rates on different substrates, it cannot explain the difference between evaporation rate of sessile and pendant drops.

The mobility of contact line can also be a potential explanation for the difference between evaporation rate of the sessile and pendant drops [15]. If we turn our attention to evaluation of the drop shape during the evaporation and consider the evaporation modes, one can seek alternative explanation for observations here, now that other possibilities are eliminated. According to Picknett and Bexon [30], for evaporation of pure sessile drops, the following two drop shape changes or a combination of them is expected: (i) decrease of wetted area with constant contact angle; and (ii) constant wetted area with decreasing contact angle. Each of these drop evolution cases is called an evaporation mode [38-40]. Evaporation of drops usually starts in the CWA mode, then switches to the CCA mode [41-43]. According to Picknett and Bexon [30] evaporation in constant wetted area (CWA) mode is faster than that in constant contact angle (CCA)

mode (by 30–40%). This is consistent with the relation between contact line and evaporation rate [44] as in the CCA mode contact line shrinks whereas in the CWA mode contact line remains constant.

As shown in Table 3, there is a meaningful difference between the time sessile and pendant drops stay in the CWA mode (same liquid type and substrate). For example, a 4 μl sessile water drop on PMMA coated silicon stays for 318 s in the CWA mode, whereas the same system but pendant stays for 274 s in the CWA mode (with 95% confidence), see Table 3. Difference between contact line motion of sessile and pendant drop is also mentioned in [15]. In [15], pendant and sessile water drops with a mixture of 1 and 3 μm polystyrene spheres evaporated at room temperature and 0% humidity. For the whole evaporation time, sessile drops evaporated in CWA mode. However, the contact line of pendant drops appeared not fixed (Devlin et al. [15] did not compare the evaporation rate of sessile and pendant drops). As evaporation rate is higher in CWA mode; this can explain why sessile drops evaporate faster than pendant drops.

Table 3 Time spent in CWA (constant wetted area) or CCA (constant contact angle) modes during the evaporation of a 4 μl water drop.

Substrate		CWA (s)	Lifetime (s)
PMMA coated silicon		318 \pm 77	1138 \pm 98
		274 \pm 40	1205 \pm 114
Aluminum		1185 \pm 61	1355 \pm 7
		1155 \pm 49	1400 \pm 71
Glass		665 \pm 42	905 \pm 49
		570 \pm 21	1040 \pm 14
PMMA coated aluminum		320 \pm 28	1445 \pm 35
		285 \pm 33	1535 \pm 62

The above result also poses an interesting question as why the pendant and sessile drops demonstrated different behavior in terms of their contact line motion during the evaporation. Some explanations are provided in [15] based on convection within the drops. But this matter can be studied in a dedicate separate study.

In summary, it was found that buoyancy is a contributor to the evaporation; however, buoyancy

alone cannot explain the difference between evaporation rate of sessile and pendant drops. The effect of buoyancy is overshadowed by drop shape evolution during the evaporation (i.e. the time spent in the CWA mode).

7. CONCLUSIONS

To have a better insight into the evaporation of sessile and pendant drops, this study examined the difference

between evaporation rate of sessile and pendant drops. It was found there is a significant difference between evaporation rates of sessile and pendant drops. Literature suggests “buoyancy” as a possible candidate for explaining the difference. By studying suspended drops near a plate, it was found that depending on the vapor’s weight and location of plate (above or underneath the drop) evaporation rate accelerated or decelerated in favor of buoyancy (which is found to be in the order of 5–8%). However, in the case of sessile and pendant drops, regardless of vapor’s weight, and on different substrates, sessile drops evaporated 16–35% faster. We showed that the buoyancy effect is overshadowed by another factor. This factor stems from the interaction of drop and surface. Because when drops were not in contact with the plate, buoyancy could explain the evaporation rate difference. The factor is found to be due to contact line dynamics of the drop during the evaporation. It was shown that sessile drops stay longer in the CWA mode compared with pendant drops, and evaporation rate in the CWA mode is (30–40%) faster than that in the CCA mode. An interesting question to be answered is as why the pendant and sessile drops demonstrated different behavior in terms of their contact line motion during the evaporation, which can be studied in future.

ACKNOWLEDGEMENT

Authors would like to thank Natural Sciences and Engineering Research Council of Canada (NSERC).

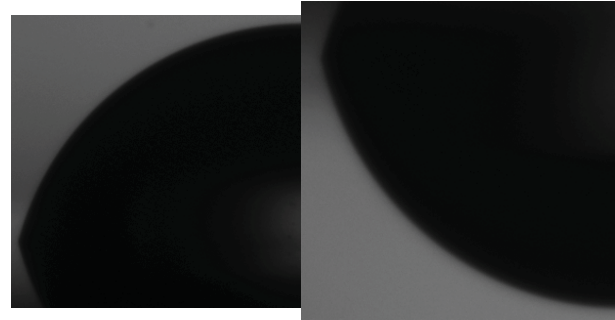
Appendix I

The initial possible shape difference is due to gravity. For micro-liter drops, the Bond number value is low, 0.019 for sessile, and 0.018 for pendant drops ($Bo = \frac{\Delta\rho g L^2}{\gamma}$, $\Delta\rho$ is the density difference between the liquid and vapor, g is the gravitational acceleration, γ is the surface tension, L is a characteristic length and is equal to $3V/S$; V is the drop volume and S is the drop surface area) [28]. As such, gravitational forces should not affect the drop’s shape, meaning that sessile and pendant drops should have the same shape (see Fig. AI-1). This is also tested using image processing methods and comparing the initial shape of similar drop volumes and surfaces in sessile and pendant configurations.

To better verify that sessile and pendant micro-liter drops have similar shapes, the sphericity (ψ) definition was used, see Eq. AI-1.

$$\psi = \frac{\pi^{1/3} (6V_s)^{2/3}}{S_s}$$

where V_s and S_s are volume and surface area of the ellipsoidal shape, accordingly, and can be found from Eqs. 3 and 4:



(a) (b)

(4) Fig. AI-4 Images of a 4 mg water drop in (a) sessile, and (b) pendant configurations on PMMA-coated silicon are shown.

$$V_s = \frac{4}{3} \pi r_1^2 r_2$$

$$S_s = 2\pi r_1^2 + \frac{2\pi r_1 r_2^2}{\sqrt{r_2^2 + r_1^2}} \sin^{-1} \frac{\sqrt{r_2^2 - r_1^2}}{r_2}$$

where r_1 and r_2 are minor and major radii of the ellipse (see Fig 7).

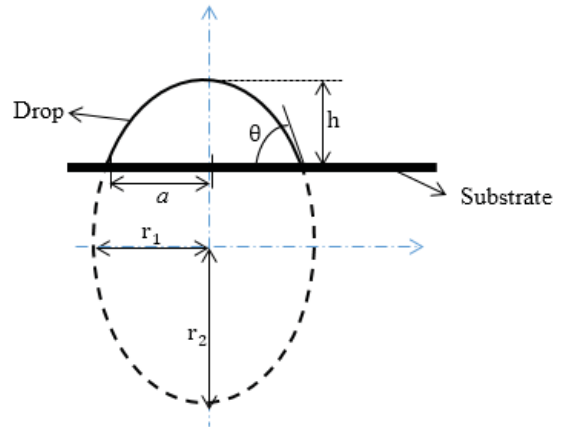


Fig. AI-5 An ellipsoidal cap shape drop with drop height (h), wetted radius (a), and contact angle (θ) is shown in 2-D. The ellipsoidal cap (which represents a drop affected by gravity) is a portion of an ellipsoid with major and minor radii of r_1 and r_2 .

A sphere has a sphericity (ψ) of unity. If drop is

affected by gravity, its shape deviates from spherical cap to an ellipsoidal cap shape [29-31], and the value of sphericity deviates from unity. Assuming that the drop is axisymmetric, one of the symmetrical axes of the ellipsoid becomes perpendicular to the substrate and the other axis of symmetry is parallel to the substrate (see Fig. 7).

The values of r_1 and r_2 cannot be measured from the drop image. Instead, the values of drop height (h), wetted radius (a), and contact angle (θ) can be found using the drop images and image processing [15]. In the following, r_1 and r_2 are found as functions of h , a , and θ . The general equation of an ellipse with minor and major radii of r_1 and r_2 is:

$$\frac{x^2}{r_1^2} + \frac{y^2}{r_2^2} = 1$$

At $x = a$, the tangent to the ellipse is θ degrees with respect to the x-axis (see Fig. 7), as such one has:

$$\left. \frac{dy}{dx} \right|_{x=a} = -\tan\theta$$

Using Eqs. 5 and 6 one can find the value of r_1 and r_2 based on the drop height (h), wetted radius (a), and contact angle (θ) as:

$$r_2 = \frac{ah \tan \theta - h^2}{a \tan \theta - 2h}$$

and:

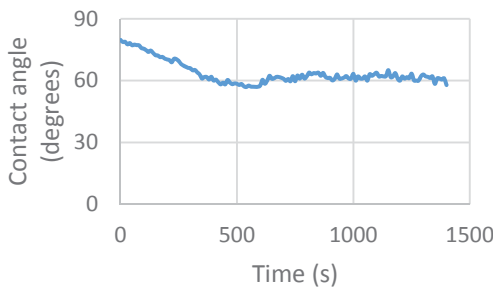
$$r_1 = \sqrt{\frac{a(a \tan \theta - h)^2}{\tan \theta (a \tan \theta - 2h)}}$$

Analyzing the drop images to find θ , a and h then r_1 and r_2 (using Eqs. 7 and 8), it was found that the sphericity of sessile and pendant water drops was 0.95 ± 0.01 and 0.96 ± 0.01 , respectively. These two values are reasonably similar which indicates that sessile and pendant drops have relatively similar shapes. Also, as the sphericity values are close to unity, it can be concluded that both sessile and pendant drops have spherical cap shapes. Above discussion shows that the initial drop shape cannot explain the difference between the evaporation of pendant and sessile drops.

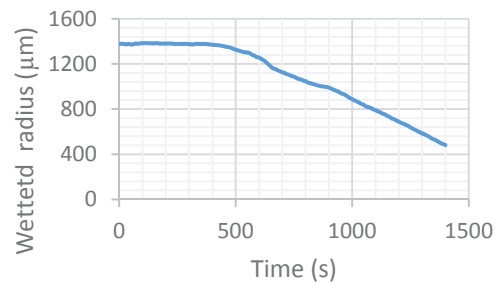
Appendix II

(5)

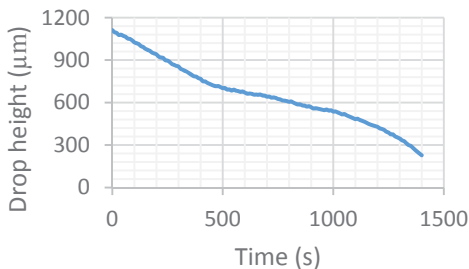
Evaporation of a 4 μl water drop on aluminum is shown. As shown below, for the first 400 s evaporation is in the constant wetted area (CWA) mode, then switches to the constant contact angle (CCA) mode.



(a)



(b)



(c)

Fig. AI-6 (a) contact angle, (b) wetted radius, and (c) drop height of a 4 μl water drop on aluminum is shown.

8. References

[1] A.C. Ihnen, A.M. Petrock, T. Chou, P.J. Samuels, B.E. Fuchs, W.Y. Lee, Crystal morphology variation in inkjet-

- printed organic materials, *Appl. Surf. Sci.* 258 (2011) 827-833.
- [2] T. Lim, S. Han, J. Chung, J.T. Chung, S. Ko, C.P. Grigoropoulos, Experimental study on spreading and evaporation of inkjet printed pico-liter droplet on a heated substrate, *International Journal of Heat and Mass Transfer*. 52 (2009) 431-441.
- [3] Y. Yu, H. Zhu, J.M. Frantz, M.E. Reding, K.C. Chan, H.E. Ozkan, Evaporation and coverage area of pesticide droplets on hairy and waxy leaves, *Biosystems Engineering*. 104 (2009) 324-334.
- [4] U. Id, Superhydrophobic Metal-Oxide Thin Film Coatings, (2012) 2012.
- [5] Z. Zhang, J. Li, P.X. Jiang, Experimental investigation of spray cooling on flat and enhanced surfaces, *Applied Thermal Engineering*. 51 (2013) 102-111.
- [6] R. Bhardwaj, X. Fang, P. Somasundaran, D. Attinger, Self-assembly of colloidal particles from evaporating droplets: role of DLVO interactions and proposition of a phase diagram. *Langmuir*. 26 (2010) 7833-42.
- [7] S. Tonini, Heat and mass transfer modeling of submicrometer droplets under atmospheric pressure conditions, *Atomization and Sprays*. 19 (2009) 833-846.
- [8] C. Poulard, G. Guéna, A. Cazabat, Diffusion-Driven Evaporation of Sessile Drops, *Journal of Physics Condensed Matter*. 17 (2005) S4213-S4227.
- [9] J.C. Maxwell, No title, in: *Anonymous Collected Scientific Papers*, 1st ed., Cambridge, 1890, pp. 628.
- [10] G. Gue'na, C. Poulard, M. Voue', J. De Coninck, A.M. Cazabat, Evaporation of sessile liquid droplets, (2006).
- [11] C. Poulard, G. Gue, A.M. Cazabat, A. Boudaoud, M.B. Amar, Rescaling the Dynamics of Evaporating Drops, (2005) 8226-8233.
- [12] S.F. Chini, A. Amirfazli, Understanding the evaporation of spherical drops in quiescent environment, 432 (2013) 82-88.
- [13] S.F. Chini, Drop Removal from Solid Surfaces: Shedding and Evaporation, (2013).
- [14] S.F. Chini, A. Amirfazli, Evaporation of Sessile Drops: Electrostatic Analogies, *Advances in Colloid and Interface Science*.
- [15] N.R. Devlin, K. Loehr, M.T. Harris, The importance of gravity in droplet evaporation: A comparison of pendant and sessile drop evaporation with particles, *AIChE Journal*. 62 (2016) 947-955.
- [16] P.L. Kelly-Zion, J. Batra, C.J. Pursell, Correlation for the convective and diffusive evaporation of a sessile drop, *International Journal of Heat and Mass Transfer*. 64 (2013) 278-285.
- [17] F. Carle, B. Sobac, D. Brutin, Experimental evidence of the atmospheric convective transport contribution to sessile droplet evaporation, *Applied Physics Letters*. 102 (2013) 061603.
- [18] S. Dehaeck, A. Rednikov, P. Colinet, Vapor-Based Interferometric Measurement of Local Evaporation Rate and Interfacial Temperature of Evaporating Droplets, *Langmuir*. 30 (2014) 2002-2008.
- [19] P.L. Kelly-Zion, C.J. Pursell, S. Vaidya, J. Batra, Evaporation of sessile drops under combined diffusion and natural convection, *Colloids Surf. Physicochem. Eng. Aspects*. 381 (2011) 31-36.
- [20] P.L. Kelly-Zion, C.J. Pursell, R.S. Booth, A.N. VanTilburg, Evaporation rates of pure hydrocarbon liquids under the influences of natural convection and diffusion, *Int. J. Heat Mass Transfer*. 52 (2009) 3305-3313.
- [21] P.L. Kelly-Zion, C.J. Pursell, N. Hasbamrer, B. Cardozo, K. Gaughan, K. Nickels, Vapor distribution above an evaporating sessile drop, *International Journal of Heat and Mass Transfer*. 65 (2013) 165-172.
- [22] P.L. Kelly-Zion, C.J. Pursell, R.S. Booth, A.N. VanTilburg, Evaporation rates of pure hydrocarbon liquids under the influences of natural convection and diffusion, *Int. J. Heat Mass Transfer*. 52 (2009) 3305-3313.
- [23] O. Carrier, N. Shahidzadeh-Bonn, R. Zargar, M. Aytouna, M. Habibi, J. Eggers, D. Bonn, Evaporation of water: evaporation rate and collective effects, *Journal of Fluid Mechanics*. 798 (2016) 774-786.
- [24] H.Y. Erbil, Evaporation of pure liquid sessile and spherical suspended drops: A review, *Advances in Colloid and Interface Science*. 170 (2012) 67-86.
- [25] D. Hu, H. Wu, Volume evolution of small sessile droplets evaporating in stick-slip mode, *Physical Review E*. 93 (2016) 042805.
- [26] T.A.H. Nguyen, A.V. Nguyen, Transient Volume of Evaporating Sessile Droplets: 2/3, 1/1, or Another Power Law? *Langmuir*. 30 (2014) 6544-6547.
- [27] R.H. Perry, D.W. Green, *Chemical Engineering Handbook*, McGraw-Hill Book Co., New York, 1997.
- [28] Y.A. Cengel, *Heat Transfer a Practical Approach*, McGraw-Hill Book Co., New York, 2003, pp. 857-868-868.
- [29] S.F. Chini, A. Amirfazli, A method for measuring contact angle of asymmetric and symmetric drops, *Colloids and Surfaces A: Physicochemical and Engineering Aspects*. 388 (2011) 29-37.
- [30] R.G. Picknett, R. Bexon, The Evaporation of Sessile or Pendant Drops in Still Air, *J. Colloid Interface Sci.* 61 (1977) 336-350.
- [31] H.K. Dhavaleswarapu, C.P. Migliaccio, S.V. Garimella, J.Y. Murthy, Experimental investigation of

evaporation from low-contact-angle sessile droplets, *Langmuir*. 26 (2010) 880-888.

[32] S. Semenov, V.M. Starov, R.G. Rubio, H. Agogo, M.G. Velarde, Evaporation of sessile water droplets: Universal behaviour in presence of contact angle hysteresis, *Colloids and Surfaces A: Physicochemical and Engineering Aspects*. 391 (2011) 135-144.

[33] H. Hu, R.G. Larson, Evaporation of a sessile droplet on a substrate, *J Phys Chem B*. 106 (2002) 1334-1344.

[34] Z.Q. Zhu, D. Brutin, Q.S. Liu, Y. Wang, A. Mourembles, J.C. Xie, L. Tadrist, Experimental investigation of pendant and sessile drops in microgravity, *Microgravity Science and Technology*. 22 (2010) 339-345.

[35] R.D. Deegan, O. Bakajin, T.F. Dupont, Capillary flow as the cause of ring stains from dried liquid drops, (1997).

[36] R.D. Deegan, O. Bakajin, T.F. Dupont, G. Huber, S.R. Nagel, T.A. Witten, Contact line deposits in an evaporating drop, *Phys. Rev. E*. 62 (2000) 756-765.

[37] R.D. Deegan, Pattern formation in drying drops, *Phys. Rev. E*. 61 (2000) 475-485.

[38] C. Bourgès-Monnier, M.E.R. Shanahan, Influence of evaporation on contact angle, *Langmuir*. 11 (1995) 2820-2829.

[39] L. Shi, P. Shen, D. Zhang, Q. Lin, Q. Jiang, Wetting and evaporation behaviors of water ethanol sessile drops on PTFE surfaces, *Surface and Interface Analysis*. 41 (2009) 951-955.

[40] R.G. Picknett, R. Bexon, The evaporation of sessile or pendant drops in still air, *J. Colloid Int. Sci*. 61 (1977) 336-350.

[41] H.Y. Erbil, G. McHale, M.I. Newton, Drop evaporation on solid surfaces: Constant contact angle mode, *Langmuir*. 18 (2002) 2636-2641.

[42] H.Y. Erbil, Evaporation of pure liquid sessile and spherical suspended drops: A review, *Adv. Colloid Int. Sci*. 170 (2012) 67-86.

[43] H.Y. Erbil, M. Dogan, Determination of diffusion coefficient-vapor pressure product of some liquids from hanging drop evaporation, *Langmuir*. 16 (2000) 9267-9273.

[44] B. Sobac, D. Brutin, Triple-line behavior and wettability controlled by nanocoated substrates: Influence on sessile drop evaporation, *Langmuir*. 27 (2011) 14999-15007.